HMG Advance Access published January 4, 2008

An *Actn3* knockout mouse provides mechanistic insights into the association between α-actinin-3 deficiency and human athletic performance

Daniel G. MacArthur,[1,2] Jane T. Seto,[1,2] Stephen Chan,[3] Kate G.R. Quinlan,[1,2] Joanna M. Raftery,[1] Nigel Turner,[4] Megan D. Nicholson,[1] Anthony J. Kee,[5] Edna C. Hardeman,[5] Peter W. Gunning,[6] Greg J. Cooney,[4] Stewart I. Head,[3] Nan Yang,[1] Kathryn N. North[1,2*]

[*]Corresponding Author:

Professor Kathryn N. North

Institute for Neuromuscular Research

The Children's Hospital at Westmead

Locked Bag 4001, Westmead, 2145

Sydney, NSW, Australia. Telephone: 61-2-9845-1906, Fax: 61-2-9845-3389

Email: kathryn@chw.edu.au

The authors wish it to be known that the first two authors should be regarded as joint First Authors

[1] Institute for Neuromuscular Research, The Children's Hospital at Westmead, Sydney, 2145 NSW, Australia

[2] Discipline of Paediatrics and Child Health, Faculty of Medicine, University of Sydney, Sydney, 2006 NSW, Australia

[3] School of Medical Sciences, University of New South Wales, Sydney, 2052 NSW, Australia

[4] Diabetes and Obesity Program, Garvan Institute of Medical Research, Darlinghurst, NSW, Australia

[5] Muscle Development Unit, Children's Medical Research Institute, Sydney, 2145 NSW, Australia

[6] Oncology Research Unit, The Children's Hospital at Westmead, Sydney, 2145 NSW, Australia

ABSTRACT

A common nonsense polymorphism (R577X) in the *ACTN3* gene results in complete deficiency of the fast skeletal muscle fiber protein α-actinin-3 in an estimated one billion humans worldwide. The XX null genotype is under-represented in elite sprint athletes, associated with reduced muscle strength and sprint performance in non-athletes, and is over-represented in endurance athletes, suggesting that α-actinin-3 deficiency increases muscle endurance at the cost of power generation. Here we report that muscle from *Actn3* knockout mice displays reduced force generation, consistent with results from human association studies. Detailed analysis of knockout mouse muscle reveals reduced fast fiber diameter, increased activity of multiple enzymes in the aerobic metabolic pathway, altered contractile properties, and enhanced recovery from fatigue, suggesting a shift in the properties of fast fibers towards those characteristic of slow fibers. These findings provide the first mechanistic explanation for the reported associations between R577X and human athletic performance and muscle function.

INTRODUCTION

The *ACTN3* gene encodes the protein α-actinin-3, a highly conserved component of the contractile machinery in fast skeletal muscle fibers (1). Remarkably, homozygosity for a common nonsense polymorphism (R577X) in the *ACTN3* gene results in complete deficiency of α-actinin-3 in ~18% of healthy individuals of European origin, with varying frequency in other populations (2, 3). We and others have previously demonstrated that the R577X polymorphism is associated with human muscle performance. The 577XX null genotype is markedly under-represented in elite sprint athletes (4, 5), and has also been associated with reduced muscle strength and sprint performance in non-athlete cohorts (6-8), suggesting that α-actinin-3 deficiency has a detrimental effect on the function of fast skeletal muscle fibers. In contrast, the XX genotype is slightly over-represented among elite female long-distance athletes (4), suggesting that α-actinin-3 deficiency may also enhance endurance performance.

Recently we described the generation and initial analysis of an *Actn3* knockout mouse model of α-actinin-3 deficiency (9), and demonstrated that loss of α-actinin-3 expression in this model results in a shift in muscle metabolism towards the more efficient aerobic pathway, and a consequently greater running distance prior to exhaustion in a motorized treadmill test. In addition, we showed that the region of genomic DNA surrounding the human 577X allele carries a signature of recent positive natural selection in European and East Asian populations, suggesting that the loss of α-actinin-3 expression was advantageous during the adaptation of modern humans to the Eurasian environment. However, insights into the biochemical and physiological effects of α-actinin-3 deficiency are required to unravel the mechanisms by which the R577X polymorphism influences human athletic performance, and precisely which phenotypes underlie selection on the 577X allele during recent human evolution.

Here we present an extensive phenotypic analysis of the *Actn3* knockout (KO) mouse. At baseline, KO mice show normal morphology, activity levels and fiber type proportions. In agreement with published results from human association studies, KO mice display a mild reduction in grip strength relative to wild-type (WT) littermate controls, and isolated KO muscles generate lower maximal force but enhanced recovery from fatigue. Detailed analysis of KO muscle reveals a number of phenotypic changes, including reduced fast fiber diameter and increased activity of a variety of enzymes typically associated with slow fiber metabolism. Physiological studies of isolated muscles demonstrate that α-actinin-3 deficiency is associated with slower twitch half-relaxation times. These findings are consistent with a shift in the properties of fast fibers towards those typically associated with slow fibers, and provide the first mechanistic explanations for the association of the 577X allele with reduced sprint/power performance but increased endurance performance in humans.

RESULTS

We have previously described the design and generation of a mouse *Actn3* null allele through a targeted deletion of exons 2-7 of *Actn3* (9). Homozygous KO mice display complete deficiency of α-actinin-3 protein by both immunohistochemistry and Western blot, and a compensatory up-regulation of the related isoform α-actinin-2. α-Actinin-2 is expressed in all muscle fibers in postnatal KO muscle, mimicking the pattern of expression in humans deficient for α-actinin-3 (10). *Actn3* KO mice thus represent an excellent model in which to study the effects of α-actinin-3 deficiency on skeletal muscle function and performance.

Morphology and behavior in KO mice is similar to WT

KO mice are morphologically indistinguishable from their wild-type (WT) littermates on gross physical inspection and general autopsy. We analyzed the general behavior and physical activity of 7-8 week-old male and female WT mice and KO littermates using an open-field test. No difference in ambulatory activity was observed over a 20 minute test period, and KO mice did not differ from WT in the time spent in peripheral or central zones, suggesting that exploratory behavior is similar in both genotypes (data not shown). KO mice also performed as well as WT in a simple rod pull-up test designed to identify severe weakness and fatigue sensitivity in mouse models of muscle disease (data not shown), indicating that any effects of α-actinin-3 deficiency on muscle function are within the limits of normal variation (11).

Grip strength is reduced in KO mice

Given the reduced muscle strength associated with α-actinin-3 deficiency in humans (6), we examined grip strength in α-actinin-3 deficient mice. Analysis of 43 male and 83 female untrained 7-9 week old mice showed that all mice produced grip strength that falls within the previously reported normal range for the related sub-strain 129S1/SvImJ (0.81-1.28N for

males; 0.81-1.16N for females (12)). However, KO mice displayed significantly lower average grip strength compared to WT mice (7.4% lower [$P = 0.007$] in males and 6.0% lower [$P = 0.02$] in females) (Fig. 1B).

Reduced total body weight, lean mass and isolated muscle mass in KO mice

We examined total body and isolated muscle mass in KO and WT mice to determine if the reduction in grip strength was attributable to a reduction in muscle size. On average, male KO mice ($n = 27$) had 4% lower total body weight than WT controls ($n = 32$); a similar effect of genotype was observed in female mice of the same age (Fig. 2A). Analysis of body composition using dual-energy X-ray absorptiometry (DEXA) analysis suggested that the lower body weight was predominantly due to lower lean mass in KO mice; no difference in fat mass was observed (Fig. 2B).

To determine the basis of this decrease in lean mass, we assessed the weights of a variety of tissues from male WT and KO mice. Internal organs including liver, kidney, lungs, brain and heart were of equivalent weights in both groups (data not shown). We also removed and weighed a variety of skeletal muscles, including the slow soleus muscle, which does not normally express α-actinin-3. All fast KO muscles analyzed, including four separate hindlimb muscles, the axial muscle spinalis thoracis, and two forelimb muscles (the biceps and triceps) weighed significantly less in KO than in WT mice (Fig. 2C). The degree of reduction in muscle mass differed depending on the location of the muscles, with the proximal muscles (quadriceps, spinalis, triceps) typically being more affected than the more distal muscles (tibialis anterior, extensor digitorum longus [EDL], gastrocnemius). In contrast to the faster muscles, the slow postural soleus muscle was heavier in KO mice compared to WT, suggesting a compensatory increase in size due to the reduced size of surrounding muscles. In isolated muscle experiments (see below) we found that muscles from KO mice had similar

optimal lengths (data not shown), demonstrating that the difference in muscle mass arises from reduced cross-sectional area (CSA) of KO muscles.

Effect of α-actinin-3 deficiency on fiber type proportions and fiber diameter

To examine the effects of α-actinin-3 deficiency on fiber type proportions and sizes, we immunostained transverse sections of quadriceps (which includes the vastus intermedius, vastus medialis and vastus lateralis), spinalis thoracis, EDL and soleus muscles for myosin heavy chains (MyHC) type 1, 2A, 2X and 2B. The muscles examined were selected to represent proximal and distal regions, while the soleus was examined as a muscle in which α-actinin-3 is usually not expressed.

The total number of fibers in the EDL muscle did not differ significantly between WT and KO mice (data not shown). In addition, analysis of fiber type proportions in the EDL, soleus and spinalis muscles revealed similar proportions of 1, 2A, 2X and 2B fibers in WT and KO muscles (Table 1). These findings indicate that the observed reduction in muscle mass in KO mice is not the result of lower total fiber number or a higher proportion of slow fibers (which are smaller in diameter than fast fibers (13), and instead suggest a specific reduction in fiber size.

To confirm this, the diameters of muscle fibers from all four fiber types were assessed in the quadriceps, spinalis, EDL and soleus (Fig. 3A-D). Fast glycolytic 2B fibers (which express α-actinin-3 in WT mice) were substantially reduced in diameter in muscles from KO mice. In the quadriceps, KO muscle fibers expressing MyHC 2B had an average diameter 34% smaller than 2B-positive fibers in WT muscle (Fig. 3A). Similar results were obtained in quadriceps of 16 week-old mice (data not shown), and also in the spinalis and EDL muscles of 8 week-old mice (Fig. 3B,C).

There was a consistent trend towards increased diameter in the other fiber types in all muscles (Fig. 3A-D), although this only reached significance for 2X fibers in the spinalis and quadriceps. This trend likely explains the increased size of the soleus muscle (which consists entirely of slow, 2A and 2X fibers) in KO mice (Fig. 2C). It is likely that the increased size of the more oxidative fiber types represents compensation for the decreased size of 2B fibers; however, the fact that KO muscles have reduced mass and generate less force than WT muscles indicates that this does not completely ameliorate the effect of decreased 2B fiber size.

Metabolic effects of α-actinin-3 deficiency

We next examined the metabolic profile of KO muscles compared to wild-type littermates. We have previously demonstrated that quadriceps muscles from KO mice display increased activity of the mitochondrial enzyme citrate synthase, and decreased activity of the anaerobic pathway enzyme lactate dehydrogenase (9). We have now extended our metabolic analysis to include a panel of enzymes representing a much broader sample of the metabolic network. The glycolytic pathway showed variable changes, with substantially increased activity for hexokinase (26%) and glyceraldehyde-6-phosphate dehydrogenase (62%) but no detectable change in the activity of phosphofructokinase. Two mitochondrial enzymes of the tricarboxylic acid (TCA) cycle (citrate synthase and succinate dehydrogenase) and one electron transport chain enzyme (cytochrome *c* oxidase) showed activity levels 25-39% higher in KO muscle relative to WT. Two mitochondrial enzymes involved in fatty acid oxidation, hydroxyacyl-CoA dehydrogenase and medium chain acyl-CoA dehydrogenase, also showed 30-42% higher activity in KO muscle, suggesting an increased reliance on β-oxidation of fatty acids in the absence of α-actinin-3 expression (Fig. 4A). Glutamate dehydrogenase, a mitochondrial enzyme that is not involved in glucose or fatty acid metabolism, had similar activity levels in WT and KO. These changes are consistent with

metabolic adaptations previously observed in endurance-trained mice and humans (14, 15). In combination these data suggest a shift in the muscle metabolism of fast fibers in KO mice away from their traditional reliance on anaerobic metabolism towards the slower but more efficient aerobic pathway.

To determine if the increase in mitochondrial enzyme levels was due to an increase in mitochondrial biogenesis, we used a quantitative PCR-based approach to assess mitochondrial DNA copy number relative to nuclear genome copy number. There was no significant difference between KO and WT littermates for this assay (Fig. 4B). There was also no detectable increase in the expression of the mitochondrial biogenesis marker *Pgc-1α* in KO muscle (data not shown). These findings suggest that higher oxidative enzyme activity in KO muscle does not arise from an increase in mitochondrial number, but instead is due to an absolute increase in mitochondrial enzyme activity.

Isolated muscle contractile properties

We analyzed isolated fast-twitch EDL muscles from WT and KO mice to identify any differences in contractile properties resulting from α-actinin-3 deficiency. KO muscles displayed significantly longer twitch half-relaxation times (time taken for muscles to relax to half of peak twitch force after a contraction) - 15.8 ± 0.6 ms in KO vs. 13.2 ± 0.6 ms in WT mice ($P = 0.007$) (Fig. 5A). This finding is consistent with a shift in the properties of the typically fast-twitch EDL muscle towards the characteristics of a slower, more oxidative muscle, and would be expected to hamper the ability to generate rapid and repetitive forceful contractions required for sprint or power performance.

An over-representation of the α-actinin-3 deficient XX genotype in endurance athletes has been previously reported (4). We thus tested the ability of isolated EDL muscles from WT and KO mice to recover following a 30-second fatigue induction protocol. Prior to fatigue,

EDL muscles from KO mice generated on average 10.9% less force than those from WT mice (Fig. 5B), consistent with the reduced grip strength values reported above. Immediately following fatigue induction both WT and KO muscles showed similar reductions in force generation capacity, but KO muscles recovered 9.8% more force generation capacity than WT after a 30 min. recovery period (Fig. 5C). The difference in recovery was most apparent at 50Hz to 100Hz activation (data not shown), corresponding to the activity that would be expected in the muscle during mid to maximal endurance running (16).

DISCUSSION

We have explored the validity of the knockout mouse as a model of XX humans by assessing two phenotypes associated with α-actinin-3 deficiency in humans: reduced muscle strength and increased endurance performance. We have replicated the human association of α-actinin-3 deficiency with lower muscle strength (6, 8) in the mouse model *in vivo* using a grip strength assay (Fig. 1), and confirmed these findings *in vitro* by demonstrating that isolated hindlimb muscles from KO mice display lower force generation capacity than those from WT (Fig. 5B). We have also replicated the association of the XX genotype with enhanced endurance performance (4); the intrinsic endurance capacity of KO mice is higher than WT (9), and isolated muscles from KO mice display enhanced recovery from contraction-induced fatigue relative to those from WT (Fig. 5C). Thus the *Actn3* knockout mouse replicates the reported effects of α-actinin-3 deficiency in humans.

Detailed analysis of *Actn3* KO mice reveals a range of phenotypic changes that provide potential mechanisms for the effect of α-actinin-3 deficiency on human performance. In wild-type mice, muscle fiber types differ from one another with respect to many functional parameters; specifically, slow fibers tend to be smaller than fast fibers (13), rely predominantly on aerobic metabolism rather than anaerobic reduction of pyruvate for energy generation, and possess distinct contractile properties including slower relaxation times (16). As a consequence of these differences, slow fibers tend to generate less force than fast fibers but are also more resistant to contraction-induced fatigue. KO muscle displays three major alterations consistent with a transformation of fast fibers towards the characteristics of slow fibers. Firstly, KO mice show a significant reduction in muscle mass, detectable by both total body weight and by isolated muscle mass (Fig. 2). This results from a marked and specific reduction in the diameter of fast glycolytic 2B fibers relative to WT muscle (Fig. 3) in the

absence of any changes in fiber type proportion (Table 1). In mouse muscle, oxidative (type 1 and 2A) fibers are consistently smaller than fast glycolytic 2B fibers (13); the decreased diameter of 2B fibers in KO mice is thus consistent with a shift towards the phenotype typical of slower fiber types. The end result of these changes is that a much smaller volume of KO muscle is composed of 2B fibers. Since 2B fibers are the major contributors to the rapid generation of muscle power (17) this change would be expected to decrease the capacity of α-actinin-3 deficient muscle to generate rapid contractile force, consistent with the association of the XX genotype with reduced muscle strength and sprint performance in humans, and with the lower grip strength and muscle force generation of KO mice.

Secondly, a wide range of enzymes characteristic of slow fiber metabolism – including components of the TCA cycle, mitochondrial electron transport chain and fatty acid oxidation pathway – display consistently higher activity in KO muscle relative to WT (Fig. 4A). These findings suggest a broad shift in the metabolic properties of knockout fast muscle fibers towards the aerobic pathway characteristic of slow fibers, concomitant with a decrease in the activity of the anaerobic pathway typically relied on for rapid muscle contraction. Consistent with this finding, KO fast-twitch muscles show enhanced force recovery from fatigue (Fig. 5B), a feature that is more characteristic of a muscle with slower fibers (18). Improved force recovery in fast fibers of KO mice would be beneficial for endurance athletes at times of fast motor unit recruitment, given that power generation and endurance performance is a "trade-off" (19) and both qualities are required in an elite endurance athlete (20).

Finally, isolated EDL muscles from KO mice display a longer twitch half-relaxation time than WT muscles (Fig. 5A), again reflecting the shift in the contractile properties of α-actinin-3-deficient 2B fibers towards those of a slower-twitch, more oxidative fiber type. Such a change is consistent with the observation that elite sprinters have a very low

frequency of α-actinin-3 deficiency: activities such as sprinting require rapid repetitive contractions, which would be hampered by prolonged relaxation times.

In summary, the muscle fibers of KO mice display alterations to three separate parameters – fast fiber cross-sectional area, metabolism and contractile properties – in a direction consistent with a shift towards the properties of slow muscle fibers, without any change in myosin heavy chain expression. The resulting phenotype closely resembles that seen following prolonged endurance training, which also results in reduced fast fiber size, increased oxidative metabolism, increased mitochondrial density and reduced shortening velocity of type 2 fibers (20). In addition, a highly similar phenotype has been reported for transgenic mice over-expressing the muscle regulatory factor myogenin (21). This raises the possibility that α-actinin-3 and myogenin act as negative and positive regulators, respectively, of a signaling pathway responsive to endurance training, which modulates both metabolism and fiber size within skeletal muscle. In this scenario, congenital deficiency of α-actinin-3 in KO mice and XX humans chronically activates this pathway, resulting in muscle that is essentially "pre-trained" for endurance performance. Given the trade-off between muscle adaptations for power generation and endurance performance (19, 20), this model would explain why α-actinin-3-deficient 577XX humans are over-represented in endurance events while performing more poorly in activities requiring rapid, forceful muscle contraction.

The *Actn3* KO mouse model recapitulates the phenotype of α-actinin-3 deficiency suggested by human association studies and has allowed us to explore the underlying molecular mechanisms, while controlling for genetic background and environmental variables such as diet and levels of activity. The *ACTN3* 577X null allele is predicted to result in α-actinin-3 deficiency in more than a billion humans world-wide (9). As such, in addition to their relevance for sporting prowess, the phenotypic consequences of α-actinin-3 deficiency – including reduced muscle mass and altered metabolic properties – may have important

implications for public health. In particular, R577X may act as a phenotypic modifier in common diseases such as age-related loss of muscle bulk (sarcopenia), and in an individual's response to exercise training and dietary regimes. The phenotypic changes observed in the mouse model can now be used to guide future genetic association studies of large cohorts of affected and unaffected human populations to assess these possibilities.

MATERIALS AND METHODS

This study was approved by our local Animal Care and Ethics Committee. All tests were performed on N4 mice of 129 genetic background, as described previously (9). All mice were fed food and water *ad libitum*, and were maintained on a 12h:12h cycle of light and dark.

Open field test

General behavior and open field activity level of 27 males (13 WT, 14 KO) and 69 females (29 WT, 40 KO) were tested over a 20-min interval using the Photobeam Activity System – Open Field (San Diego Instruments) during their light cycle between 9am-2pm. Mice were isolated during testing to avoid human interference in their movements and behavior. The resulting movements of each mouse were recorded as fine movements, ambulation and rearing, where fine movements were defined as repeated breaks of the same beam within a set time interval; ambulation defined as breaks of multiple beams within the same set time interval; and rearing as beam breaks at the Z (vertical) dimension. The total number of movements for each category were tallied for each mouse and averaged within each genotype. Movements within central and peripheral zones were similarly recorded and the mean taken for comparison between genotypes.

DEXA analysis

Whole animals were placed in a GE Lunar Piximus2 (Lunar, Madison, WI) research Dual Energy X-ray Absorptiometry (DEXA) scanner for scanning, calibrated using a hydroxy-apatite “phantom” mouse model provided by the supplier. Data analysis was performed using the manufacturer’s software with default settings. Lean and fat mass were calculated using the entire mouse body and limbs and excluding the head and tail.

Grip strength

Mouse forearm grip strength was tested using a grip strength meter (Columbus Instruments). Mice were lifted by the base of the tail and allowed to grasp the trapeze with their front paws. During the test, mice were pulled perpendicularly from the meter whilst keeping the body parallel to the floor. Results were recorded in newtons (N). Each mouse was trialed ten times; an extra five trials were added if the mouse failed to properly grasp the trapeze during the test, or relinquished its hold before any force was applied, resulting in ambiguous readings that were ±0.3N from previous trials. For these reasons, the lowest reading was not included in the final analysis of the data. The highest reading was likewise excluded to control for operator error, since higher readings can be erroneously obtained if the meter is not properly tared before the commencement of each trial. The remaining readings for each mouse were averaged; a total of 53 males (19 WT; 24 KO) and 83 females (39 WT; 44 KO) were tested to derive the mean grip strength for each genotype. All mice were tested by operators blinded to genotype.

Rod Pull-Up Test

Whole animal muscle strength was tested according to Hubner et al, (1996) (11). Briefly, mice were suspended on a rod (3mm diameter) by their front paws and allowed to pull themselves up. Success in lifting the whole body onto the rod within 2 seconds was rated as a pass; failure to lift the whole body within 2 seconds was rated as a fail. Each mouse was trialed 15 times within a 3-minute period. Muscle strength was defined as the average pass rate over the 15 trials.

Tissue collection

Mice were euthanized by cervical dislocation immediately prior to tissue collection. Muscles and organs were removed, weighed, and immediately snap-frozen in liquid nitrogen (for

metabolic enzyme analysis) or covered in cryo-preservation medium (Tissue-Tek) and frozen in partly-thawed isopentane. Tissue was stored in liquid nitrogen until use.

Immunohistochemistry

Transverse 8 μm sections were cut from the mid-section of frozen quadriceps, spinalis, EDL and soleus muscles. All sections were blocked with AffiniPure Fab fragment goat anti-mouse IgG (1:25 dilution; Jackson ImmunoResearch) for one hour to prevent cross-reaction with endogenous mouse antibodies. Sections were incubated overnight at 4^{o}C with monoclonal antibodies from hybridoma cultures to detect MyHC isoforms 2A (undiluted SC71), 2B (undiluted BF-F3) and 2X (undiluted 6H1-2A) (antibodies kindly supplied by J. Hoh and E. Hardeman). MyHC isoform 1β was detected with MAB1628 (1:300 dilution; Chemicon). All samples were co-stained with dystrophin (dys6-10; 1:2000 dilution; kindly supplied by L. Kunkel) to define the sarcolemma for the determination of fiber borders. Following incubation with primary antibodies, sections were washed twice with 1x PBS and re-blocked with 2% BSA for 10 min prior to incubation with Cy3-conjugated affiniPure goat anti-mouse IgG (1:250 dilution; Jackson ImmunoResearch), Alexa Fluor 555 goat anti-mouse IgM (1:250 dilution; Molecular Probes) and Alexa Fluor 488 goat anti-mouse IgG (1:200 dilution; Molecular Probes) for one hour at room temperature. All samples were washed twice with 1x PBS prior to mounting to remove non-specific binding of secondary antibodies. All images were captured using ProgRes camera and software (SciTech)

Fiber diameter measurement and fiber type proportions

The fiber 'diameter' was defined as the length of the longest chord perpendicular to the longest distance that stretches through the centre of the fiber, as previously described by Song *et al.* (22). Fiber diameters were measured using Image-Pro 2.0 software (Media Cybernetics, Silver Spring, MD); mean diameter for each muscle was used for comparison between WT

and KO. All fibers were assessed for EDL and soleus. Because of processing artifacts and clustered fiber type distribution within the quadriceps, representative type 2X and 2B fibers (200-400 fibers) were assessed from the mid-belly of the vastus intermedius from each sample, while type 2A and 1 fibers were sampled from the superficial regions of vastus medialis. Similarly, fibers were sampled from the mid-region of the spinalis. Fiber type proportions were determined as the percentage of positive fibers of the total fibers in a given field. For the EDL and soleus, the proportion of positive staining fibers was relative to the total number of fibers within each muscle. For the spinalis, proportions were derived from assessments of 240-365 fibers within the mid-belly region of the muscle.

Isolated muscle analysis

Animals aged 8 to 10 weeks were anesthetized with halothane and sacrificed by cervical dislocation. The extensor digitorum longus (EDL) muscle was dissected from the hindlimb and tied by its tendons to a force transducer (World Precision Instruments, Fort 10) at one end and a linear tissue puller (University of New South Wales) at the other, using silk suture (Deknatel 6.0). It was placed in a bath continuously superfused with Krebs solution, with composition (mM): 4.75 KCl, 118 NaCl, 1.18 KH_2PO_4, 1.18 $MgSO_4$, 24.8 $NaHCO_3$, 2.5 $CaCl_2$ and 10 glucose, with 0.1% fetal calf serum and continuously bubbled with 95% O_2-5% CO_2 to maintain pH at 7.4. The muscle was stimulated by delivering a supramaximal current between two parallel platinum electrodes, using an electrical stimulator (A-M Systems). At the start of the experiment, the muscle was set to the optimum length L_0 that produced maximum twitch force. All experiments were conducted at room temperature (~22 to 24 °C).

The muscle was then stimulated with a supramaximal pulse of 1 ms duration and the resulting twitch recorded. The twitch data was smoothed by averaging the raw data over 2.5 ms

intervals, and from the resulting smoothed data the time-to-peak and the half-relaxation time were obtained.

A force-frequency curve was then obtained by delivering 500 ms stimuli of different frequencies (2, 15, 25, 37.5, 50, 75, 100, 125 and 150 Hz), and measuring the force produced at each frequency of stimulation. A 30 second rest was allowed between each frequency. A curve relating the muscle force P to the stimulation frequency f was fitted to these data. The curve had the following equation:

$$P = P_{\min} + \frac{P_{\max} - P_{\min}}{1 + \left(\frac{K_f}{f} \right)^h}$$

The values of r^2 for the fitting procedure were never lower than 0.993. From the fitted parameters of the curve, the following contractile properties were obtained: maximum force ($P_{\max}$), half-frequency (K_f), Hill coefficient (h) and twitch-to-tetanus ratio ($P_{\min}/P_{\max}$).

Finally, the muscle was removed from the bath and weighed. An estimate of the cross-sectional area was obtained by dividing the muscle's mass by the product of its optimum length and the density of mammalian muscle (1.06 mg/mm^3).

In a separate set of experiments using different muscles from those used for eccentric contractions, muscles were examined for their responses to a fatiguing protocol. Muscles were set up as described above and a force frequency curve was obtained as described above, except that the duration of stimulation at each frequency was only 250 ms. After 5 minutes, the fatigue protocol was started. The muscle was given a one-second, 100-Hz tetanus every 2 seconds over a period of 30 seconds. The muscle was then allowed to recover for a period of 30 minutes, during which force recovery was monitored with a brief (250 ms) 100-Hz tetanus every 5 minutes. Additional force-frequency curves were obtained 90 seconds after the end of the fatigue protocol, and 1 minute after the final recovery tetanus.

Enzyme assays

The activity of a number of enzymes in WT and KO muscles were determined spectrophotometrically using methods based on those of Houle-Leroy et al (2000) (14) and Turner et al (2007) (23) and references therein.

Extracts were prepared from the quadriceps muscle of seven 8 week old female 129X1/SvJ WT mice and seven 8 week old female KO mice (on a 129X1/SvJ background). Mice were sacrificed by cervical dislocation, quadriceps muscles were dissected out and were snap frozen in liquid nitrogen.

For the glyceraldehyde-3-phosphate dehydrogenase assay, 20% w/v homogenates were generated. Muscles were processed on ice using a dounce homogeniser, in 20 mM HEPES buffer, pH 7.2, containing 0.2% (v/v) Triton X-100, 1 mM EDTA, 1 mM DTT and 1 x protease inhibitor cocktail (Sigma, P-8340). Crude extracts were centrifuged at 2000g for 5 minutes at 4°C and the supernatants were sonicated.

For the remaining enzyme assays, 5% w/v homogenates were generated using a Polytron instrument at low speed in 50 mM Tris-HCl buffer, pH 7.4, containing 0.1% (v/v) Triton X-100 and 1 mM EDTA. Muscle homogenates were subjected to three freeze-thaw cycles and then were centrifuged at 13000rpm for 10 minutes at 4°C.

Glyceraldehyde-3-phosphate dehydrogenase (GAPDH, EC 1.2.1.12), lactate dehydrogenase (LDH, EC 1.1.1.27), 3-hydroxyacyl-CoA dehydrogenase (BHAD, EC 1.1.1.35) and glutamate dehydrogenase (GDH, EC 1.4.1.2) activities of extracts were measured spectrophotometrically by assessing the rate of NADH oxidation at 340 nm ($\varepsilon = 6.22\ mM^{-1}cm^{-1}$) by modifications of the methods of Heinz and Friemuller (1982) (24) Reichmann et al (1983) (25) and Anno et al (2004) (26), respectively. GAPDH assays were conducted in 30 mM Tris-HCl buffer, pH 7.5, 5 mM $MgSO_4$, 4 mM L-cysteine, 200 µM NADH, 2 mM ATP,

3 mM glycerate 3-phosphate and 10.7 U/mL 3-phosphoglycerate kinase enzyme (from yeast, Sigma, P-7634) and started by the addition of glycerate 3-phosphate. LDH assays were conducted in 10 mM potassium phosphate buffer, pH 7.2, 2 mM pyruvate and 200 μM NADH and started by the addition of pyruvate. BHAD assays were conducted in 50 mM Imidazole buffer, pH 7.4, 1.2 mM EDTA, 0.18 mM NADH and 0.1 mM acetoacetyl-CoA and started by the addition of acetoacetyl-CoA. GDH assays were conducted in 10 mM Tris-HCl buffer, pH 8.0, 10 μM EDTA, 0.1 mM NADH, 50 mM NH_4SO_4 and 5 mM α-ketoglutarate and started by the addition of α-ketoglutarate.

Citrate synthase (CS, EC 4.1.3.7) activity of extracts was measured spectrophotometrically by assessing the rate of production the 2-nitro-5-thiobenzoate anion at 412 nm ($\varepsilon = 13.6\ mM^{-1}cm^{-1}$) by a modification of the method of Srere et al (1969) (27). Assays were conducted in 100 mM Tris-HCl, pH 8.2, 300 μM acetyl CoA, 1 mM $MgCl_2$, 1 mM EDTA, 0.1 mM 5,5'-dithio-bis (2-nitrobenzoic acid) (DTNB) and 500 μM oxaloacetate and started by the addition of oxaloacetate.

Cytochrome *c* oxidase (CCO, EC 1.9.3.1) activity of extracts was measured spectrophotometrically by assessing the rate of cytochrome c oxidation at 550 nm ($\varepsilon = 19.1\ mM^{-1}cm^{-1}$). CCO assays were conducted in 100 mM KH_2PO_4/K_2HPO_4 buffer, pH 7.4 and 0.1 mM cytochrome *c* reduced with sodium hydrosulfite ($Na_2S_2O_4$), pH 7.0 and started by the addition of reduced cytochrome *c*.

Medium chain acyl-CoA dehydrogenase (MCAD, EC 1.3.99.3) activity of extracts was measured spectrophotometrically by assessing the reduction of ferricenium hexafluorophosphate ($FcPF_6$) at 300 nm ($\varepsilon = 4.3\ mM^{-1}cm^{-1}$). Assays were conducted in 100 mM KH_2PO_4/K_2HPO_4 buffer, pH 7.2, 1 mM EDTA, 0.5 mM sodium tetrathionate, 0.2 mM $FcPF_6$ and 50 μM octanoyl-CoA and started by the addition of octanoyl-CoA.

Hexokinase (HK, EC 2.7.1.1) activity of extracts was measured spectrophotometrically by assessing the rate of NADP reduction at 340 nm ($\varepsilon = 6.22\ mM^{-1}cm^{-1}$). Assays were conducted in 50 mM Imidazole, pH 7.4, 9 mM ATP, 9 mM $MgCl_2$, 0.6 mM NADP, excess levels of glucose-6-phosphate dehydrogenase (4 U) and 5 mM glucose and started by the addition of glucose.

Phosphofructokinase (PFK, 2.7.1.11) activity of extracts was measured spectrophotometrically by assessing the rate of NADH oxidation at 340 nm ($\varepsilon = 6.22\ mM^{-1}cm^{-1}$). Assays were conducted in 50 mM Imidazole, pH 7.4, 6 mM $MgCl_2$, 60 mM KCl, 5 mM ATP, 0.4 mM NADH, excess aldolase (1 U), excess triosephosphate isomerase (50 U), excess α-glycerophosphate dehydrogenase (8 U) and 5 mM fructose-6-phosphate and started by the addition of fructose-6-phosphate.

Succinate dehydrogenase (SDH, 1.3.5.1) activity of extracts was measured spectrophotometrically by assessing the rate of 2,6-dichlorophenol-indophenol (DCIP) reduction at 600 nm ($\varepsilon = 21\ mM^{-1}cm^{-1}$). Assays were conducted in 50 mM KH_2PO_4/K_2HPO_4 buffer, pH 7.0, 20 mM succinate, 2.5 μM antimycin A, 2.5 mM KCN, 0.45 mM phenazine methosulphate (PMS), 0.12 mM DCIP and started by the addition of DCIP.

For all assays the linearity with time and dependence on the amount of extract added were confirmed. All assays for a particular enzyme were performed on the same day. The same volume of each sample extract was used for each assay. Activity of GAPDH over a 1 minute period was assayed at 23 °C in triplicate. Activities for each sample in the absence of substrate were measured for each sample and were subtracted from these values. The triplicate readings for each sample were averaged. For the rest of the enzymes, assays were performed at 30 °C in duplicate which were averaged.

Total protein content of extracts for GAPDH assays were measured using the Pierce BCA™ Protein Assay Kit (23227), according to the manufacturer's instructions, for BSA standards and extracts in triplicate. Total protein content of extracts for the remainder of the assays were measured using the BioRad Protein Assay (500-0006), according to the manufacturer's instructions, for BSA standards and extracts in duplicate. The mg protein in each extract was used to convert the activities of each enzyme (mU) to specific activities (mU/mg or nmol/min/mg protein).

qPCR analysis

Mitochondrial DNA (mtDNA) copy number: We performed Quantitative PCR (qPCR) analysis using the Corbett Rotor-Gene 3000™ to compare the mtDNA content of quadriceps muscles harvested from 4 WT and 4 α-actinin-3 KO mice. Total DNA was extracted from ~ 50 mg frozen muscle using QIAamp DNA Mini Kit Tissue Protocol (Qiagen). The LUX™ Primer Design System (Invitrogen) was used to design primers for the single-copy mitochondrial gene *mt-Rnr2* (16S rRNA; 5'-CGGGAGAATTACAGCTAGAAACCC-[FAM]G-3'; 5'-GCTATCACCAAGCTCGTTAGGC-3') and the 2-copy nuclear gene *Rn18S* (18S rRNA; 5'-CGGCACTTTCGATGGTAGTCGC[FAM]G-3'; 5'-GGTCGGGAGTGGGTA-ATTTGC-3'). Calibration curves were generated for the genomic and mitochondrial genes from a serial dilution of DNA harvested from WT quadriceps run concurrent to unknown samples, and used to determine the relative amount of each gene in KO and WT quadriceps. The amount of mtDNA to the amount of nuclear DNA was normalized for each sample before expressing the level of mtDNA present in α-actinin-3 KO mice as a percentage of that identified in WT littermates.

Pgc-1α expression levels: Total RNA was extracted from 3 WT and 3 KO frozen, sectioned gastrocnemius using Tri-Reagent (Molecular Research Centre Inc), and cDNA synthesized using random primers (Invitrogen) and reverse transcriptase SuperScript III (Invitrogen)

according to the instructions of the manufacturer. qPCR was performed using primers specific for the *Pgc-1α* transcript (peroxisome proliferative activated receptor, gamma, coactivator 1 alpha; 5'- CGGTCTATGGTTCTGAGTGCTAAGAC[FAM]G-3'; 5'-CAACGAGGCCAGTCCTTCCT-3'), and the transcript of the endogenous reference gene *Hprt1* (hypoxanthine guanine phosphoribosyl transferase 1; 5'-AGCCCCAAAATGGTT-AAGGTT[FAM]G-3'; 5'-CTGGCCTGTATCCAACACTTCG-3') (The LUX™ Primer Design System; Invitrogen). Standard curves were prepared by cloning the target sequences into plasmids, and data was analyzed as instructed in the Rotor-Gene protocol.

Statistics

All comparisons reported in this study involved small sample sizes to which standard tests for normality could not be applied. As such, all comparisons of means were performed using the non-parametric Mann-Whitney U test. All histograms show mean values, with error bars indicating 95% confidence intervals (95% CI) unless otherwise stated.

ACKNOWLEDGMENTS

We thank M. Nair (The Children's Hospital at Westmead) for assistance in fiber diameter data collection. This project was funded in part by a grant (301950) from the Australian National Health and Medical Research Council. D.G.M. and J.T.S. were supported by Australian Postgraduate Awards.

AUTHOR CONTRIBUTIONS

D.G.M. and N.Y. generated the knockout mouse. J.T.S. analyzed the morphology, behavior and grip strength of knockout mice; J.T.S., M.D.N., J.M.R. and N.Y. performed the analysis for fiber diameter and fiber type proportions; S.C. and S.I.H. performed the contractility studies; K.G.Q., N.T. and G.J.C. performed the metabolic analyses; J.M.R and N.Y. designed and performed qPCR analyses; J.M.R. maintained the mouse line; D.G.M., J.T.S., J.M.R., K.G.Q. and N.Y. collected muscle weight data and harvested muscles for analysis; A.J.K., E.C.H., and P.W.G. provided expertise in analysis of mouse phenotype; D.G.M. and K.N. designed the study; D.G.M., J.T.S. and K.N. wrote the manuscript.

CONFLICT OF INTEREST STATEMENT

The authors have no conflicts of interest to declare.

REFERENCES

1. MacArthur, D.G. and North, K.N. (2004) A gene for speed? The evolution and function of alpha-actinin-3. *Bioessays,* **26,** 786-795.
2. Mills, M., Yang, N., Weinberger, R., Vander Woude, D.L., Beggs, A.H., Easteal, S. and North, K. (2001) Differential expression of the actin-binding proteins, alpha-actinin-2 and -3, in different species: implications for the evolution of functional redundancy. *Hum. Mol. Genet.,* **10,** 1335-1346.
3. Yang, N., MacArthur, D.G., Wolde, B., Onywera, V.O., Boit, M.K., Lau, S.Y.M., Wilson, R.H., Scott, R.A., Pitsiladis, Y.P. and North, K.N. (2007) The ACTN3 R577X polymorphism in east and west African athletes. *Med. Sci. Sports Exerc.,* **39,** 1985-1988.
4. Yang, N., MacArthur, D.G., Gulbin, J.P., Hahn, A.G., Beggs, A.H., Easteal, S. and North, K. (2003) ACTN3 genotype is associated with human elite athletic performance. *Am. J. Hum. Genet.,* **73,** 627-631.
5. Niemi, A.K. and Majamaa, K. (2005) Mitochondrial DNA and ACTN3 genotypes in Finnish elite endurance and sprint athletes. *Eur. J. Hum. Genet.,* **13,** 965-969.
6. Clarkson, P.M., Devaney, J.M., Gordish-Dressman, H., Thompson, P.D., Hubal, M.J., Urso, M., Price, T.B., Angelopoulos, T.J., Gordon, P.M., Moyna, N.M. *et al.* (2005) ACTN3 genotype is associated with increases in muscle strength in response to resistance training in women. *J. Appl. Physiol.,* **99,** 154-163.
7. Moran, C.N., Yang, N., Bailey, M.E., Tsiokanos, A., Jamurtas, A., MacArthur, D.G., North, K., Pitsiladis, Y.P. and Wilson, R.H. (2007) Association analysis of the ACTN3 R577X polymorphism and complex quantitative body composition and performance phenotypes in adolescent Greeks. *Eur. J. Hum. Genet.,* **15,** 88-93.

8. Vincent, B., De Bock, K., Ramaekers, M., Van den Eede, E., Van Leemputte, M., Hespel, P.J. and Thomis, M. (2007) The ACTN3 (R577X) genotype is associated with fiber type distribution. *Physiol. Genomics*, 10.1152/physiolgenomics.00173.2007

9. MacArthur, D.G., Seto, J.T., Raftery, J.M., Quinlan, K.G., Huttley, G.A., Hook, J.W., Lemckert, F.A., Edwards, M.R., Berman, Y., Hardeman, E.C. *et al.* (2007) Loss of function of the ACTN3 gene alters muscle metabolism in a mouse model and has been favored by selection during recent human evolution. *Nat. Genet.,* **39,** 1261-1265.

10. North, K.N., Yang, N., Wattanasirichaigoon, D., Mills, M., Easteal, S. and Beggs, A.H. (1999) A common nonsense mutation results in alpha-actinin-3 deficiency in the general population. *Nat. Genet.,* **21,** 353-354.

11. Hubner, C., Lehr, H.A., Bodlaj, R., Finckh, B., Oexle, K., Marklund, S.L., Freudenberg, K., Kontush, A., Speer, A., Terwolbeck, K. *et al.* (1996) Wheat kernel ingestion protects from progression of muscle weakness in mdx mice, an animal model of Duchenne muscular dystrophy. *Pediatr. Res.,* **40,** 444-449.

12. Kitten, A.M., Griffey, S., Chang, F., Dixon, K., Browne, C., Clary, D. and Multi-system analysis of mouse physiology. MPD:151. Mouse Phenome Database Web Site, The Jackson Laboratory, Bar Harbor, Maine USA. World Wide Web (URL: http://www.jax.org/phenome, July 2007)

13. Hamalainen, N. and Pette, D. (1993) The histochemical profiles of fast fiber types IIB, IID, and IIA in skeletal muscles of mouse, rat, and rabbit. *J. Histochem. Cytochem.,* **41,** 733-743.

14. Houle-Leroy, P., Garland, T., Jr., Swallow, J.G. and Guderley, H. (2000) Effects of voluntary activity and genetic selection on muscle metabolic capacities in house mice Mus domesticus. *J. Appl. Physiol.,* **89,** 1608-1616.

15. Phillips, S.M., Green, H.J., Tarnopolsky, M.A., Heigenhauser, G.J. and Grant, S.M. (1996) Progressive effect of endurance training on metabolic adaptations in working skeletal muscle. *Am. J. Physiol.,* **270,** E265-272.

16. McArdle, W.D., Katch, F.I. and Katch, V.L. Exercise Physiology: Energy, Nutrition, and Human Performance. 5th Edition. Lippincott, Williams & Wilkins.

17. Bottinelli, R., Pellegrino, M.A., Canepari, M., Rossi, R. and Reggiani, C. (1999) Specific contributions of various muscle fibre types to human muscle performance: an in vitro study. *J. Electromyogr. Kinesiol.,* **9,** 87-95.

18. Brotto, M.A., Nosek, T.M. and Kolbeck, R.C. (2002) Influence of ageing on the fatigability of isolated mouse skeletal muscles from mature and aged mice. *Exp. Physiol.,* **87,** 77-82.

19. Wilson, R.S. and James, R.S. (2004) Constraints on muscular performance: trade-offs between power output and fatigue resistance. *Proc. Biol. Sci.,* **271 Suppl 4,** S222-225.

20. Tanaka, H. and Swensen, T. (1998) Impact of resistance training on endurance performance. A new form of cross-training? *Sports Med.,* **25,** 191-200.

21. Hughes, S.M., Chi, M.M., Lowry, O.H. and Gundersen, K. (1999) Myogenin induces a shift of enzyme activity from glycolytic to oxidative metabolism in muscles of transgenic mice. *J. Cell Biol.,* **145,** 633-642.

22. Song, S.K., Shimada, N. and Anderson, P.J. (1963) Orthogonal Diameters in the Analysis of Muscle Fibre Size and Form. *Nature,* **200,** 1220-1221.

23. Turner, N., Bruce, C.R., Beale, S.M., Hoehn, K.L., So, T., Rolph, M.S. and Cooney, G.J. (2007) Excess lipid availability increases mitochondrial fatty acid oxidative capacity in muscle: evidence against a role for reduced fatty acid oxidation in lipid-induced insulin resistance in rodents. *Diabetes,* **56,** 2085-2092.

24. Heinz, F. and Freimuller, B. (1982) Glyceraldehyde-3-phosphate dehydrogenase from human tissues. *Methods Enzymol.,* **89 Pt D,** 301-305.

25. Reichmann, H., Srihari, T. and Pette, D. (1983) Ipsi- and contralateral fibre transformations by cross-reinnervation. A principle of symmetry. *Pflugers Arch.,* **397,** 202-208.

26. Anno, T., Uehara, S., Katagiri, H., Ohta, Y., Ueda, K., Mizuguchi, H., Moriyama, Y., Oka, Y. and Tanizawa, Y. (2004) Overexpression of constitutively activated glutamate dehydrogenase induces insulin secretion through enhanced glutamate oxidation. *Am. J. Physiol. Endocrinol. Metab.,* **286,** E280-285.

27. Srere, P.A. (1969) Citrate Synthase. *Methods Enzymol.,* **13,** 3-11

LEGENDS TO FIGURES

Figure 1. KO mice display reduced grip strength compared to WT. Grip strength assays were performed on 7-9 week old male (WT $n = 19$, KO $n = 24$) and female (WT $n = 39$, KO $n = 44$) mice. Mean ± 95% CI; $^{**}P < 0.01$.

Figure 2. KO mice show reduced total body weight, lean mass and isolated muscle mass compared to WT. **(a)** Total body weight of 7-9 week old male (WT $n = 27$, KO $n = 32$) and female (WT $n = 34$, KO $n = 36$) mice. **(b)** Total lean and fat mass determined by DEXA analysis of 8 week old male mice (WT $n = 17$, KO $n = 11$). **(c)** Mean muscle mass of extensor digitorum longus (EDL), soleus (SOL), medial biceps (BIC), triceps (TRIC), tibialis anterior (TA), gastrocnemius (GST), quadriceps (QUAD) and spinalis thoracis (SPN) excised from male 8 week old mice. Note that the three smallest muscles are shown with a separate axis to increase visual clarity. For BIC and TRIC, WT $n = 9$, KO $n = 7$; for all other muscles, WT $n = 18$, KO $n = 13$. Mean ± 95% CI; $^{*}P < 0.05$, $^{**}P < 0.01$, $^{***}P < 0.001$.

Figure 3. KO fast muscles display a trend towards reduced fast 2B diameters and increased 2X diameters relative to WT. Fiber diameters were measured in **(a)** quadriceps; **(b)** spinalis **(c)** extensor digitorum longus and **(d)** slow muscle soleus. Note lack of 2B fibers in the soleus. All graphs show mean ± 95% CI; WT and KO $n = 4$-7 for all fiber types. $^{*}P < 0.05$, $^{**}P < 0.01$.

Figure 4. KO mouse quadriceps muscles display a metabolic shift with decreased activity of anaerobic metabolism and increased activity of both glycolytic and mitochondrial aerobic enzymes occurring in the absence of increased mitochondrial DNA. **(a)** Enzyme activities of hexokinase (HK), glyceraldehyde-3-phosphate dehydrogenase (GAPDH), hexokinase (HK),

lactate dehydrogenase (LDH), citrate synthase (CS), succinate dehydrogenase (SDH), cytochrome *c* oxidase (CCO), 3-hydroxyacyl-CoA dehydrogenase (BHAD), medium chain acyl-CoA dehydrogenase (MCAD) and glutamate dehydrogenase (GDH) were determined (WT $n = 8$, KO $n = 8$). **(b)** Relative copy number of mitochondrial to nuclear DNA was determined using qPCR (WT $n = 4$, KO $n = 4$). All graphs show mean ± 95% CI. *$P < 0.05$, **$P < 0.01$, ***$P < 0.001$.

Figure 5. Isolated KO extensor digitorum longus (EDL) displayed characteristics of a "slower" fiber, with **(a)** longer half-relaxation times (mean ± SEM, WT $n = 8$, KO $n = 10$); **(b)** reduced force generation (mean ± 95% CI, WT $n = 8$, KO $n = 10$); and **(c)** enhanced force recovery following fatigue compared to WT (mean ± 95% CI, WT $n = 6$, KO $n = 8$). *$P < 0.05$, **$P < 0.01$.

Table 1. No changes in myosin heavy chain isoform proportion in either WT or KO extensor digitorum longus, soleus and spinalis. Numbers represent mean % ± 95% CI (*n*).

MyHC isoform	WT	KO	*P*-value
Extensor Digitorum longus			
IIB	58.5 ± 3.7 (5)	63.5 ± 3.5 (6)	0.126
IIX	34.7 ± 5.4 (5)	32.7 ± 2.5 (6)	0.931
IIA	19.9 ± 5.8 (5)	19.9 ± 4.6 (6)	1.000
I(β)	11.0 ± 4.6 (4)	10.3 ± 1.6 (6)	0.905
Soleus			
IIB	ND	ND	-
IIX	68.5 ± 9.3 (6)	57.9 ± 11.5 (6)	0.310
IIA	41.1 ± 6.4 (6)	44.7 ± 3.7 (6)	0.485
I(β)	43.6 ± 9.0 (6)	47.4 ± 8.3 (6)	0.699
Spinalis*			
IIB	61.3 ± 7.3 (6)	73.3 ± 6.7 (7)	0.051
IIX	31.1 ± 6.5 (6)	30.0 ± 7.4 (7)	0.628
IIA	23.9 ± 9.9 (6)	19.3 ± 6.5 (7)	0.445
I(β)	8.5 ± 3.5 (6)	8.8 ± 3.9 (7)	1.000

ND = Not detected; *Proportions for the spinalis were derived from assessments of 240-365 fibres within the mid-belly region of the muscle.

Figure 1

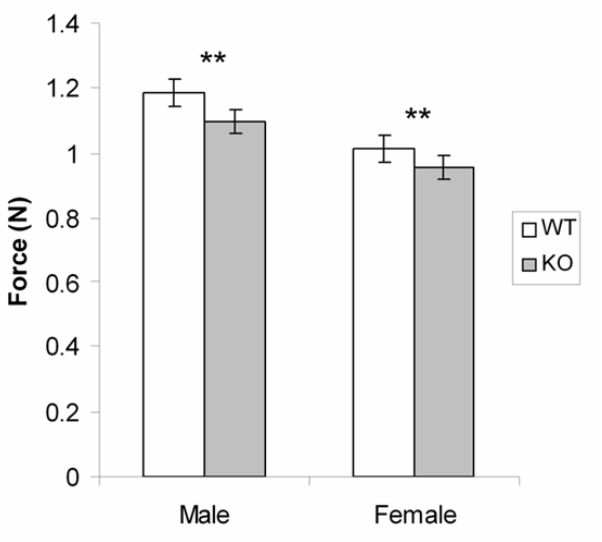

Figure 2

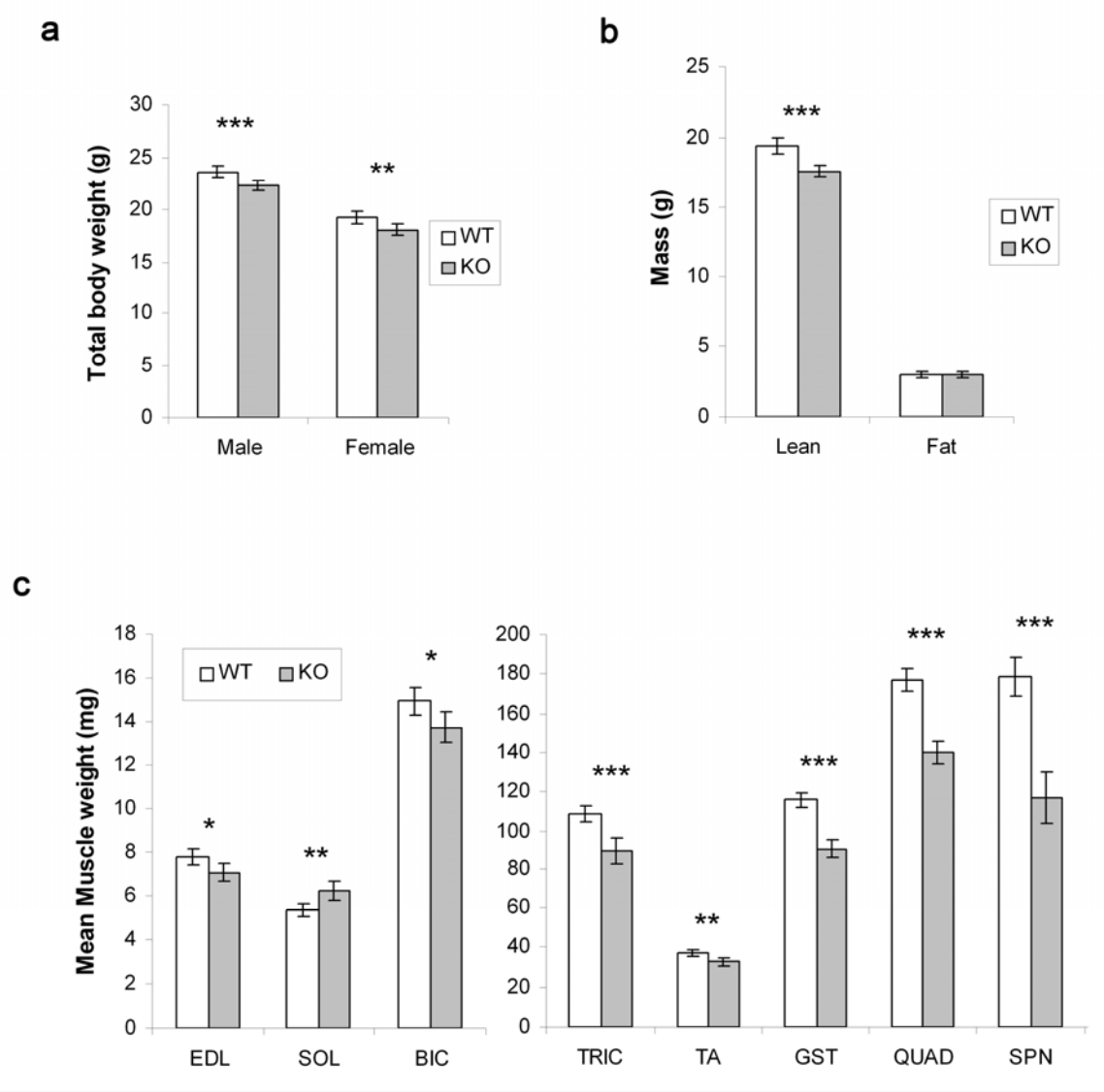
a
Total body weight (g)
30
25
20
15
10
5
0
***
**
WT
KO
Male
Female
b
Mass (g)
25
20
15
10
5
0
***
WT
KO
Lean
Fat
c
Mean Muscle weight (mg)
18
16
14
12
10
8
6
4
2
0
WT
KO
*
**
*
EDL
SOL
BIC
200
180
160
140
120
100
80
60
40
20
0
***
**
***
***
***
TRIC
TA
GST
QUAD
SPN

Figure 3

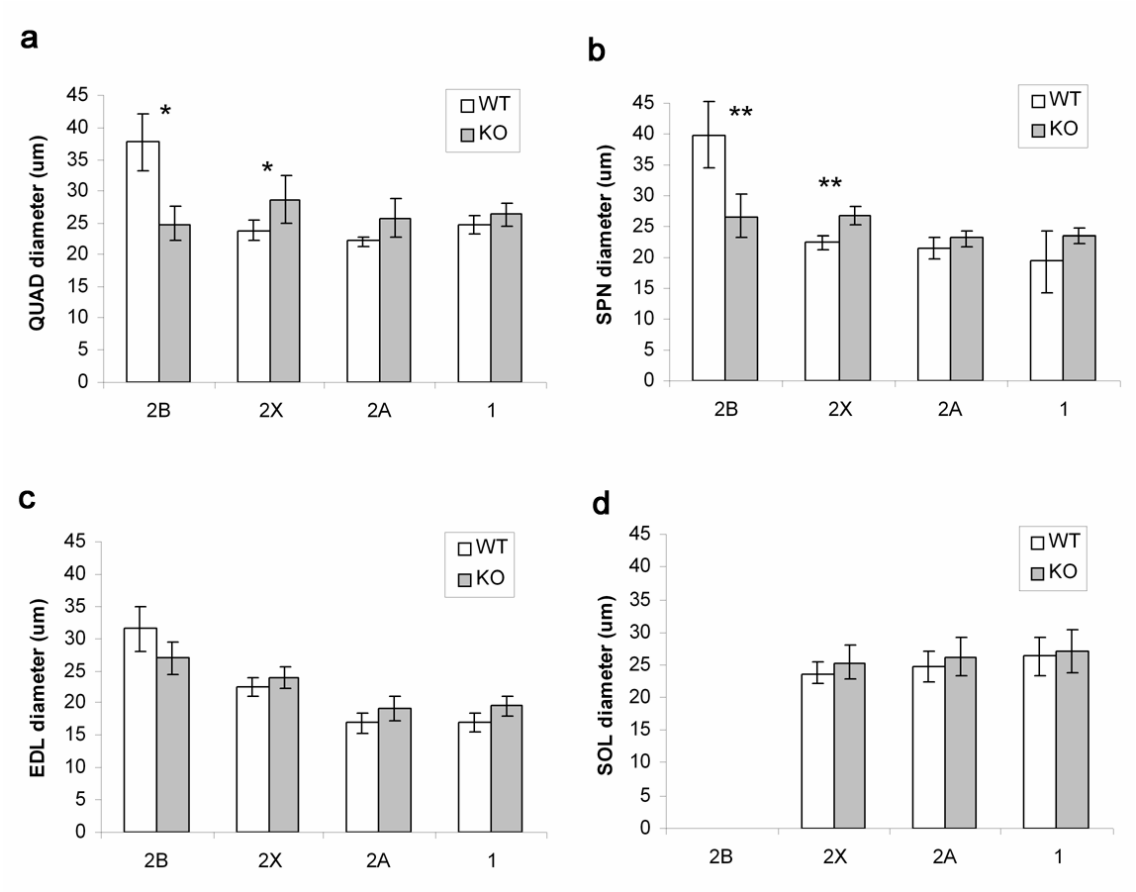
a
QUAD diameter (um)
WT
KO
*
*
2B
2X
2A
1
b
SPN diameter (um)
**
**
c
EDL diameter (um)
d
SOL diameter (um)

Figure 4

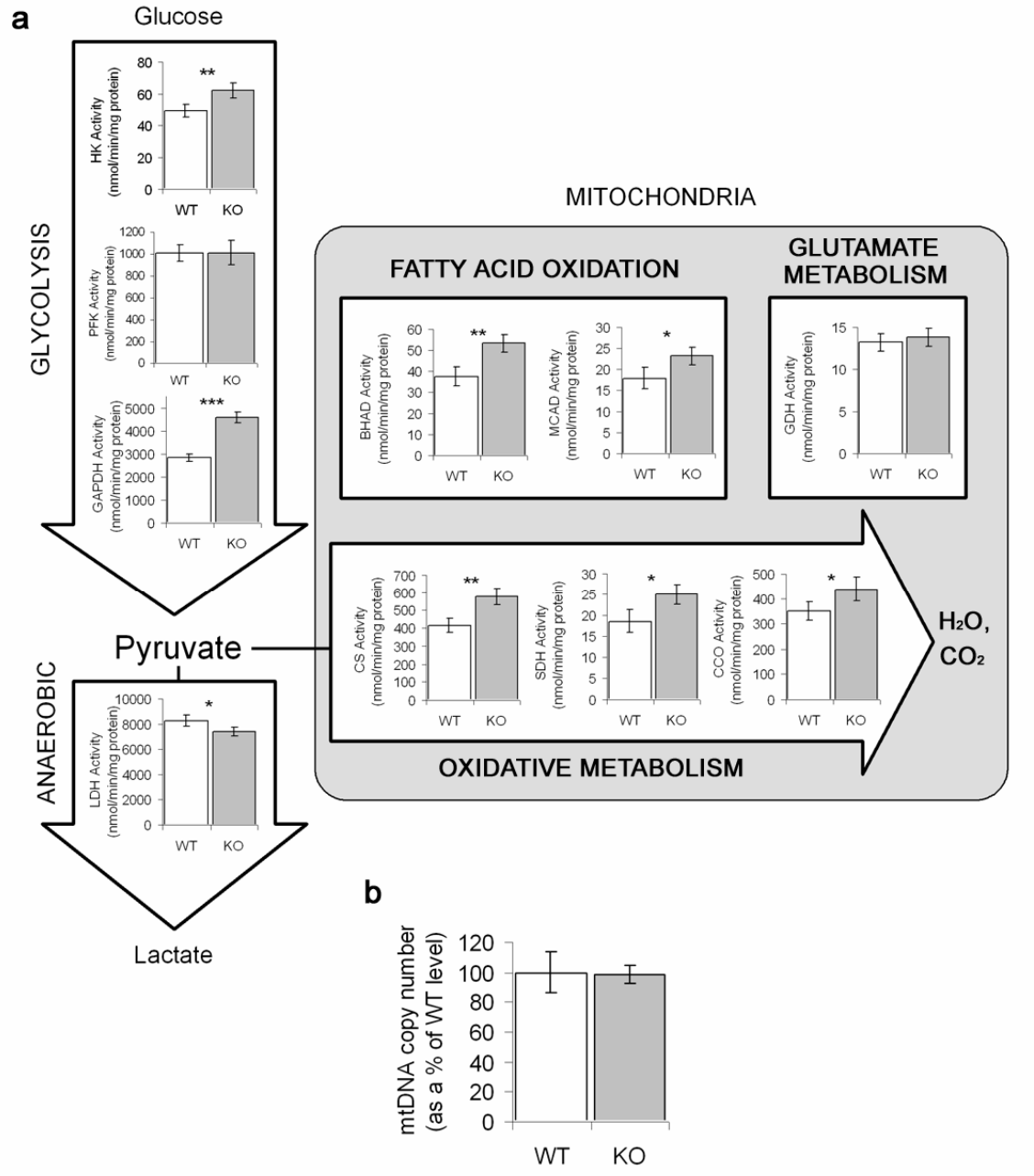
a
Glucose
GLYCOLYSIS
HK Activity (nmol/min/mg protein)
PFK Activity (nmol/min/mg protein)
GAPDH Activity (nmol/min/mg protein)
WT
KO
Pyruvate
ANAEROBIC
LDH Activity (nmol/min/mg protein)
Lactate
MITOCHONDRIA
FATTY ACID OXIDATION
BHAD Activity (nmol/min/mg protein)
MCAD Activity (nmol/min/mg protein)
GLUTAMATE METABOLISM
GDH Activity (nmol/min/mg protein)
CS Activity (nmol/min/mg protein)
SDH Activity (nmol/min/mg protein)
CCO Activity (nmol/min/mg protein)
OXIDATIVE METABOLISM
H₂O, CO₂
b
mtDNA copy number (as a % of WT level)

Figure 5

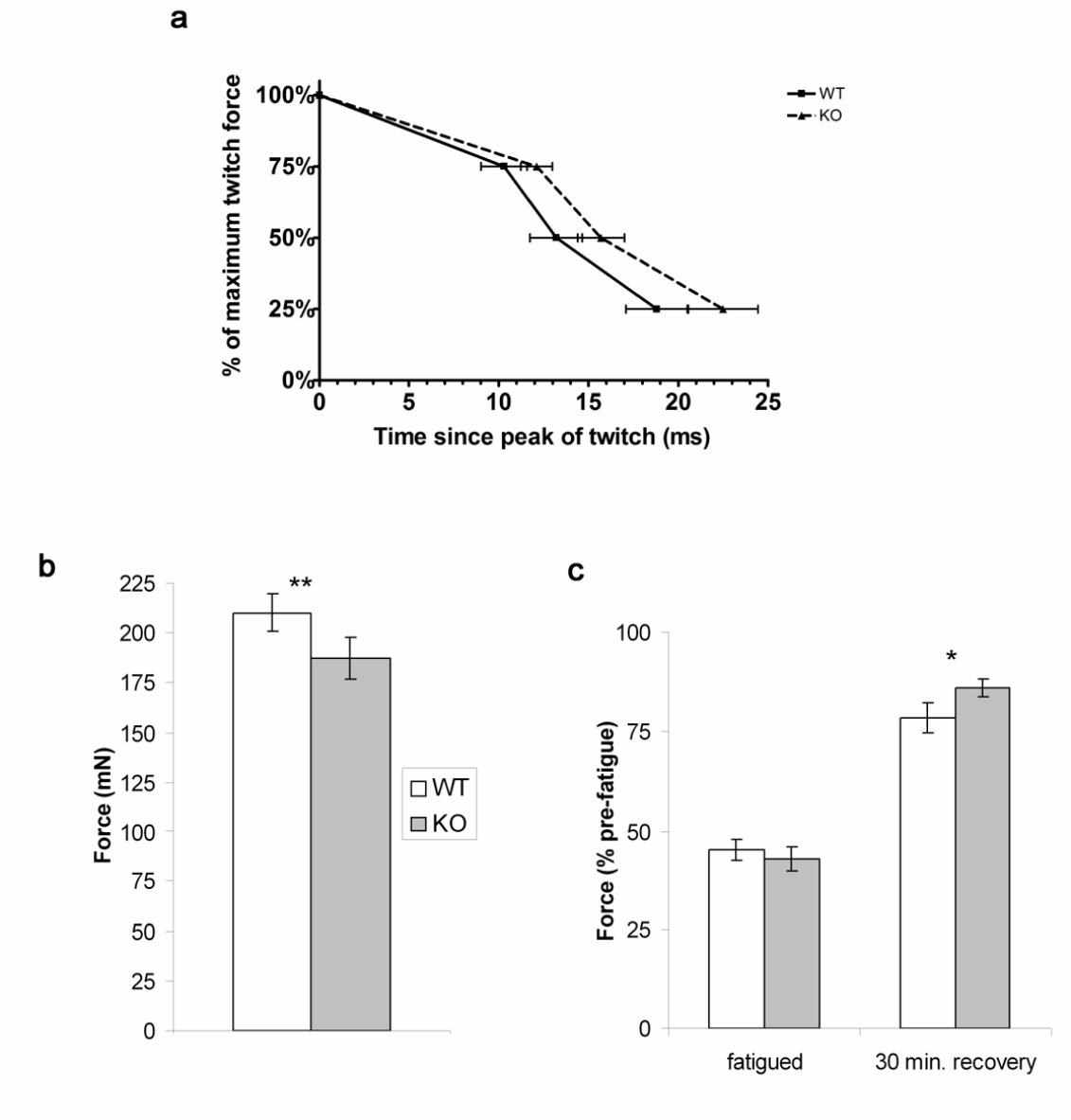
a
% of maximum twitch force
100%
75%
50%
25%
0%
0
5
10
15
20
25
Time since peak of twitch (ms)
WT
KO
b
Force (mN)
225
200
175
150
125
100
75
50
25
0
**
WT
KO
c
Force (% pre-fatigue)
100
75
50
25
0
*
fatigued
30 min. recovery